The EMBO Journal Vol. 21 No. 22 pp. 6083–6094, 2002

Syndapins integrate N-WASP in receptor-mediated endocytosis

Michael M.Kessels and Britta Qualmann[1]

Department of Neurochemistry and Molecular Biology, Leibniz Institute for Neurobiology, Brenneckestraße 6, D-39118 Magdeburg, Germany

[1]Corresponding author
e-mail: qualmann@ifn-magdeburg.de

Syndapins are potential links between the cortical actin cytoskeleton and endocytosis because this family of dynamin-associated proteins can also interact with the Arp2/3 complex activator N-WASP. Here we provide evidence for involvement of N-WASP interactions in receptor-mediated endocytosis. We reveal that the observed dominant-negative effects of N-WASP are dependent exclusively on the proline-rich domain, the binding interface of syndapins. Our results therefore suggest that syndapins integrate N-WASP functions in endocytosis. Both proteins co-localize in neuronal cells. Consistent with a crucial role for syndapins in endocytic uptake, co-overexpression of syndapins rescued the endocytosis block caused by N-WASP. An *in vivo* reconstitution of the syndapin–N-WASP interaction at cellular membranes triggered local actin polymerization. Depletion of endogenous N-WASP by sequestering it to mitochondria or by introducing anti-N-WASP antibodies impaired endocytosis. Our data suggest that syndapins may act as important coordinators of N-WASP and dynamin functions during the different steps of receptor-mediated endocytosis and that local actin polymerization induced by syndapin–N-WASP interactions may be a mechanism supporting clathrin-coated vesicle detachment and movement away from the plasma membrane.

Keywords: actin cytoskeleton/dynamin/PACSIN/syndapin/vesicle formation

Introduction

Endocytosis is critical for a variety of functions in eukaryotic cells. Moreover, endocytic pathways are exploited by viruses and other microorganisms. Vesicle formation during receptor-mediated endocytosis involves complex structural and regulatory machinery (reviewed in Schmid, 1997; Brodin *et al*., 2000; Slepnev and De Camilli, 2000). This complex machinery may also interact with the cortical actin cytoskeleton, which underlies the plasma membrane and may play a variety of roles during the different stages of an endocytic event (for a review, see Qualmann *et al*., 2000). This is supported by genetic analyses in yeast (Riezman *et al*., 1996) and ongoing identifications of mammalian proteins, which would have the potential to integrate endocytic and cytoskeletal functions, such as profilin, HIP1R, syndapins, Abp1, intersectin and cortactin. Additionally, the GTPase dynamin, which is involved in the endocytic fission reaction, and synaptojanin, which plays an important role in clathrin-coated vesicle uncoating, are implicated in cytoskeletal organization (reviewed in Qualmann and Kessels, 2002).

In order to understand how the endocytic machinery functionally interconnects with the cortical cytoskeleton, it is crucial to unravel the molecular basis of this connection. As potential links, we discovered syndapins, a family of dynamin-associated proteins. The dynamin interaction of syndapins, a family of proteins also called PACSINs (Plomann *et al*., 1998), and the fact that a surplus of the syndapin SH3 domain inhibits transferrin uptake in HeLa cells (Qualmann and Kelly, 2000) strongly implicate syndapins in endocytic function. The SH3 domain-mediated block of receptor-mediated endocytosis occurred specifically in the dynamin-controlled scission step in *in vitro* reconstitution assays (Simpson *et al*., 1999). Interestingly, overexpression of full-length syndapins causes the formation of actin-rich filopodia at the cell surface (Qualmann and Kelly, 2000). It is possible that syndapins affect the actin cytoskeleton via their binding partner N-WASP (Qualmann *et al*., 1999), the more ubiquitously expressed homologue of the Wiskott–Aldrich syndrome protein (WASP) (Miki *et al*., 1996), both potent activators of the Arp2/3 (actin-related protein 2/3) complex, which promotes actin filament formation and branching (reviewed in Higgs and Pollard, 1999). Syndapin-induced filopodia formation was found to be dependent on proper function of the Arp2/3 complex (Qualmann and Kelly, 2000). It remained unaddressed, however, whether an interaction of syndapins with the Arp2/3 complex activator N-WASP would play a role in endocytosis or solely represent a cytoskeletal function of syndapins independent from their role in endocytosis. In this study, we show that N-WASP interactions are involved in endocytosis: we find that N-WASP-derived protein tools capable of interfering with the syndapin–N-WASP interaction block receptor-mediated endocytosis. Consistently, this phenotype can be rescued by co-overexpressing syndapins. We also demonstrate that reconstituting syndapin–N-WASP complexes *in vivo* leads to local F-actin polymerization, a possible mechanism for supporting clathrin-coated vesicle detachment and movement away from the donor membrane. In line with this, endocytic uptake was found to be impaired under conditions where N-WASP was depleted by sequestration to mitochondria or by introduction of anti-N-WASP immunoreagents.

Results

Syndapin and N-WASP co-localize in hippocampal neurons

We have shown previously that N-WASP and syndapin I can exist in a complex in rat brain homogenates (Qualmann *et al*., 1999; Qualmann and Kelly, 2000), but it remained unclear whether syndapin–N-WASP protein interactions play a role in endocytosis or whether the endocytic and cytoskeletal roles of syndapins represent independent functions.

We first generated antibodies to determine the endogenous localization of N-WASP. Our affinity-purified guinea pig antibody P337 detected haemagglutinin (HA)-tagged N-WASP (Figure 1A) as specifically and efficiently as the monoclonal anti-HA antibody (Figure 1B) in COS-7 cells expressing both low and high levels of N-WASP. In immunoblot analyses, the affinity-purified P337 recognized green fluorescent protein (GFP)–N-WASP in extracts from transfected HEK cells (Figure 1C, lane 2) with the same affinity and specificity as monoclonal anti-GFP antibodies (Figure 1C, lane 4). In addition, affinity-purified P337 recognized endogenous N-WASP with an apparent mol. wt of ~70 kDa in extracts from HEK cells (Figure 1C, lanes 1 and 2) as well as in brain homogenates (Figure 1D, lane 1); P337 serum and rabbit serum 3495 gave similar results (Figure 1D, lanes 2 and 3). Endogenous N-WASP generally was found to be of low abundance but it was readily detectable in growth cones of developing neurones (Figure 1E). Here, a co-localization with both actin (our unpublished data) and syndapin was observed (Figure 1G). Additionally, N-WASP (Figure 1F) and syndapin I (Figure 1H) co-localized in varicosities of neurones at the onset of synaptogenesis. These sites are also enriched for other proteins involved in membrane trafficking processes (Qualmann *et al*., 1999; our unpublished data). Consistently, both syndapin I and N-WASP immunoreactivity was detected in the synaptosomal fraction—known to correspond to the nerve terminal region—isolated from brain tissue by differential centrifugation (Figure 1I).

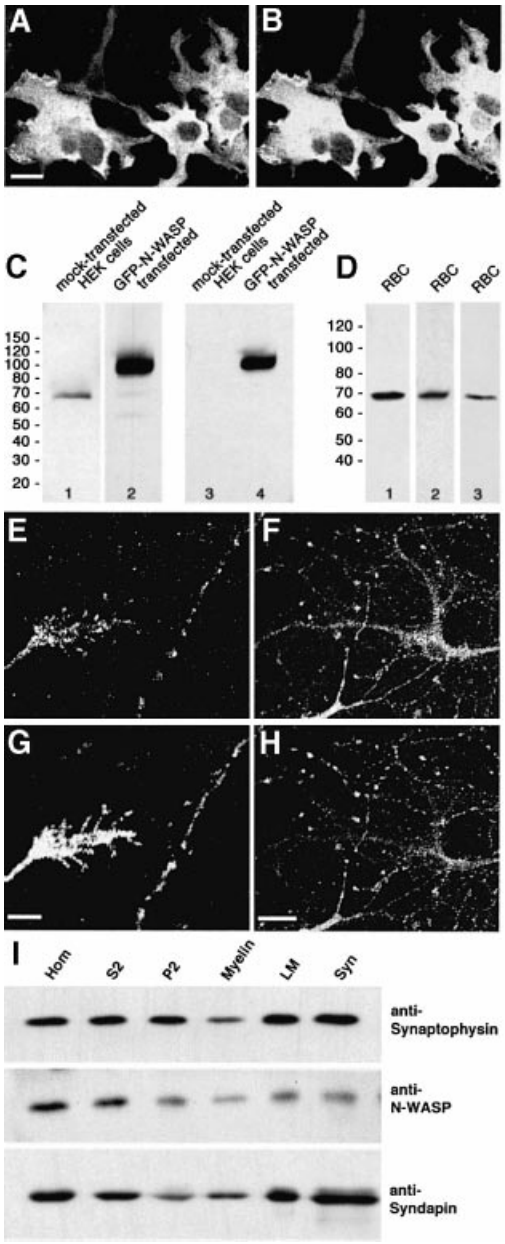

Fig. 1. Syndapins and N-WASP co-localize in growth cones and varicosities of hippocampal neurones. (A and B) Affinity-purified anti-N-WASP antibodies (P337) (**A**) recognize HA-tagged rat full-length N-WASP expressed in COS-7 cells with the same specificity as monoclonal anti-HA antibodies (**B**). (**C**) Lysates from HEK cells either mock-transfected (lanes 1 and 3) or transfected with GFP–N-WASP (lanes 2 and 4) were probed with tag-specific antibodies (anti-GFP, lanes 3 and 4) or affinity-purified P337 antibodies (lanes 1 and 2). (**D**) Affinity-purified P337 (lane 1) as well as the sera P337 (lane 2) and 3495 (lane 3) recognize a single 70 kDa band in rat brain extracts. (**E**–**H**) Syndapin I (G and H) and N-WASP (E and F) co-localize in growth cones (E and G) and varicosities (F and H) in hippocampal neurones cultured for 2 (E and G) and 9 days (F and H), respectively. Scale bars = 20 μm in (A) and (H), and 5 μm in (G). (**I**) N-WASP and syndapin I are both present in synaptosomal preparations. Western blots of rat brain homogenate (Hom), soluble fraction (S2), crude membrane fraction (P2), myelin fraction (Myelin), light membrane fraction (LM) and synaptosomal fraction (Syn) were probed with antibodies against synaptophysin, N-WASP and syndapin I.

N-WASP interactions are involved in receptor-mediated endocytosis

In order to test an involvement of N-WASP protein interactions in endocytosis, as suggested by the subcellular distribution of N-WASP in neurones (Figure 1), we analysed the uptake of fluorescently labelled transferrin in COS-7 cells transfected with N-WASP constructs (Figure 2). All HA-tagged N-WASP constructs used for this purpose throughout this study are depicted in Figure 2A. Overexpression of full-length N-WASP had a significant effect on receptor-mediated endocytosis (Figure 2B and C). Quantifications of the results of the assays revealed that <50% of the transfected cells took up transferrin similarly to wild-type cells. Almost a quarter of the cells showed a complete block of uptake (Figure 2H).

N-WASP is a multidomain protein, which interacts with several molecules. Among those are phosphatidylinositol-(4,5)-bisphosphate (PIP_2), calmodulin and the GTPase Cdc42, molecules that all have been suggested to play important roles in different endocytic processes. In order to identify the interactions crucial for receptor-mediated endocytosis, we overexpressed the respective N-WASP domains. Overexpression of a combination of the

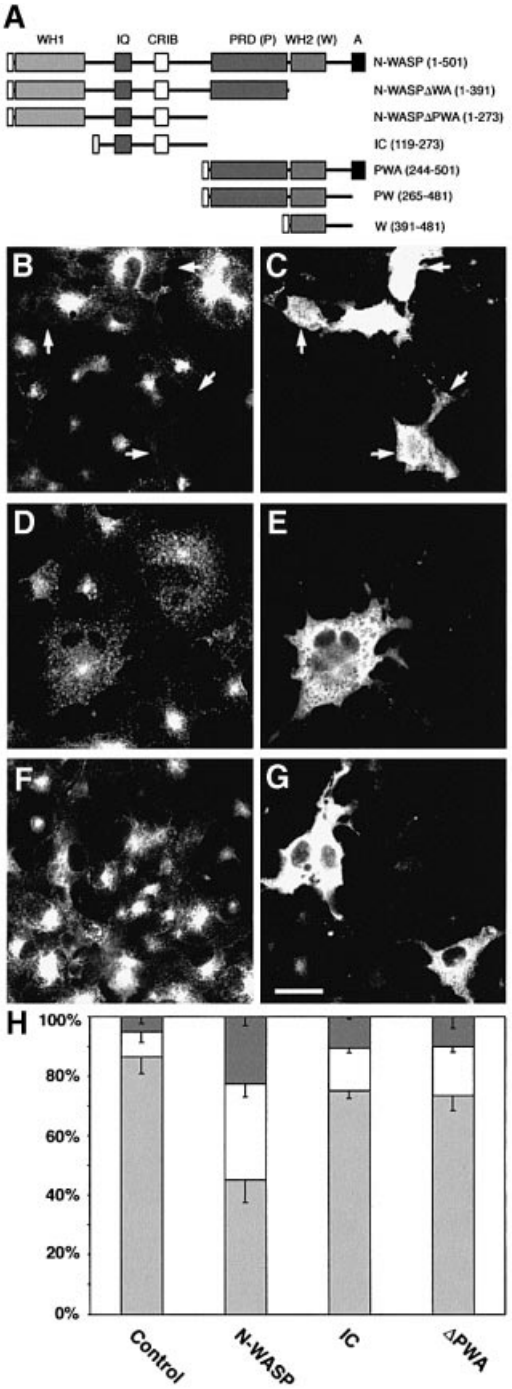

Fig. 2. N-WASP overexpression impairs receptor-mediated endocytosis. (**A**) Schematic overview of all HA-tagged N-WASP constructs used in the endocytosis assays. (B–G) Images from COS-7 cells transiently transfected with HA-tagged full-length N-WASP (**B** and **C**), IC (**D** and **E**) and N-WASPΔPWA (**F** and **G**), respectively, were recorded by confocal microscopy after an incubation with FITC–transferrin (B, D and F) for 30 min. Expression of N-WASP constructs was visualized with anti-HA antibodies (C, E and G). Arrows in (B) and (C) indicate N-WASP-overexpressing cells with strongly impaired transferrin uptake. Scale bar = 30 μm. (**H**) Quantitation of the results by assessing the percentages of cells lacking transferrin signal (block; dark grey), displaying significantly reduced levels of uptake (white) and showing endocytosis capabilities similar to untransfected cells (light grey). Untransfected cells, n = 333; N-WASP, n = 401; IC, n = 326; N-WASPΔPWA, n = 334.

calmodulin-binding IQ domain (Miki *et al*., 1996) and the Cdc42-binding CRIB domain (Miki *et al*., 1998) did not cause any effects on receptor-mediated uptake (Figure 2D and E); neither did overexpression of the CRIB domain alone (our unpublished data). Similarly, we failed to detect any inhibitory effects in cells overexpressing the entire N-terminal half of the protein (N-WASPΔPWA) including the PIP_2-binding N-terminus of the protein (Miki *et al*., 1996) (Figure 2F and G). The visual analyses were corroborated by quantitative examinations (Figure 2H). We concluded that the dominant-negative effect on endocytosis was caused by a region within the C-terminal half of N-WASP.

N-WASP interactions mediated by the PRD are responsible for the endocytosis block induced upon overexpression

We confirmed our above conclusion by overexpressing the N-WASP PWA domain. As shown in Figure 3A, overexpression of this C-terminal half of N-WASP indeed caused a strong dominant-negative effect on receptor-mediated endocytosis. It even exceeded that observed for the full-length protein, as revealed by quantitations of the results (Figure 3E). About half of all transfected cells showed a block of transferrin uptake and almost another quarter of the cells showed reduced internalization. Since overexpression of the PWA (Figure 3A) and the PW domains (Figure 3B) led to a potent block of receptor-mediated endocytosis but that of the W domain alone did not (Figure 3C), it seemed that the PRD of N-WASP was responsible for the observed phenotype. We were unable to confirm this conclusion directly, because all constructs encoding the PRD alone that we designed failed to be expressed. In order to exclude that a PRD/W domain combination is responsible for the strong endocytosis block, we analysed a combination of the non-inhibitory N-terminus (Figure 2) and the PRD (construct N-WASPΔWA). Overexpression of this construct also led to a strong block of endocytosis (Figure 3D and E). Thus, the N-WASP PRD blockes endocytosis irrespective of whether N- or C-terminal domains accompany it, suggesting that it is solely responsible for the observed dominant-negative effect on receptor-mediated endocytosis.

Syndapin binds directly to the PRD of N-WASP

We next asked whether the target of the dominant-negative effect of the N-WASP PRD on endocytosis could be syndapin, because syndapins are part of high molecular weight protein complexes in brain homogenates, which also contain N-WASP. Since neither affinity purifications, gel filtration studies nor immunoprecipitations (Qualmann *et al*., 1999) can reveal whether the syndapin–N-WASP interaction is direct, we attempted to rebuild this interaction in nuclei of yeast cells by yeast two-hybrid analyses. As shown in Figure 4A, co-expression of AD–syndapin fusion proteins together with BD–N-WASP fusion proteins led to a strong activation of the reporter genes, as analysed by β-galactosidase assays and by robust growth on drop-out plates. Importantly, this interaction was detected with all syndapin isoforms and splice variants examined. In order to prove formally that no additional molecules are required for the syndapin–N-WASP interaction, we overlaid blots from extracts

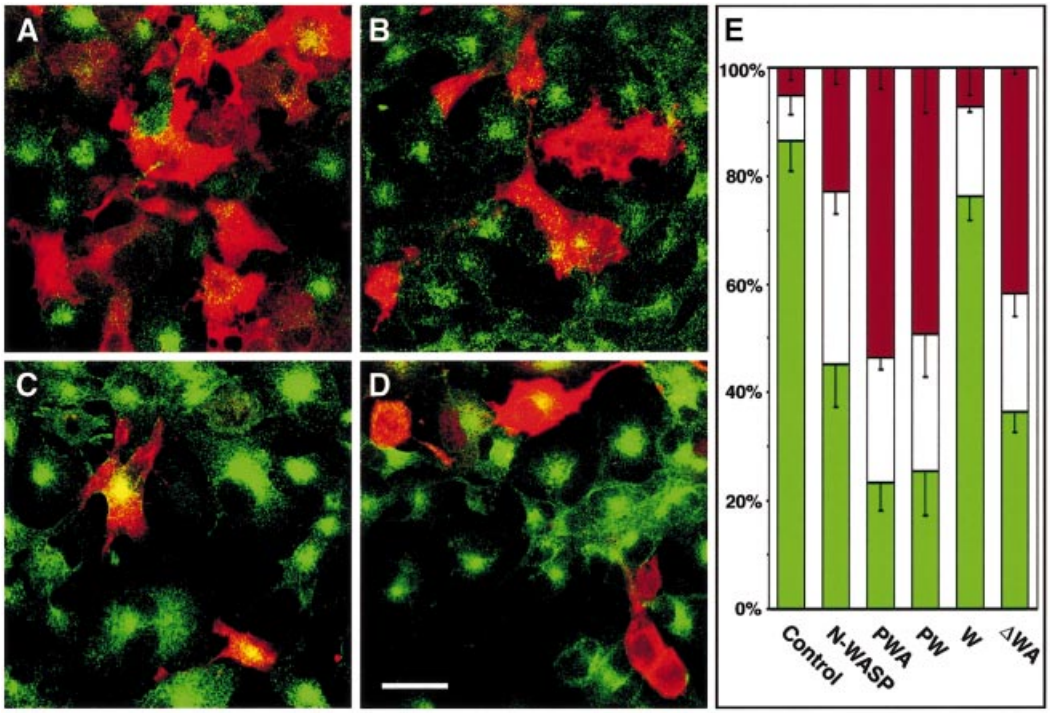

Fig. 3. The block of receptor-mediated endocytosis caused by N-WASP overexpression is due to the proline-rich domain. (A–D) Superimposition of FITC–transferrin on staining of the HA-epitope tagged N-WASP fragments. Images were recorded by confocal microscopy from COS-7 cells overexpressing the N-WASP fragments PWA (**A**), PW (**B**), W (**C**) and N-WASPΔWA (**D**), respectively. Scale bar = 30 μm. (**E**) Quantitation of the results by assessing the percentages of cells lacking transferrin signal (block, red), displaying significantly reduced levels of uptake (white) and showing endocytosis capabilities similar to untransfected cells (green). Untransfected cells, n = 333; N-WASP, n = 401; PWA, n = 357; PW, n = 399; W, n = 254; N-WASPΔWA, n = 439.

from N-WASP-transfected and untransfected cells with purified GST–syndapin I SH3 domain. The recombinant N-WASP was readily detected by this probe, demonstrating that the syndapin–N-WASP interaction is indeed direct (Figure 4B).

We next mapped which domain of N-WASP mediated the interaction with syndapin by pull-down assays using extracts from HEK cells expressing different N-WASP fusion proteins (Figure 4C). All constructs containing the PRD of N-WASP bound to immobilized syndapin SH3 domain, while all constructs without this domain did not (Figure 4D). Thus, there was a complete overlap between N-WASP constructs interfering with transferrin uptake upon overexpression (Figures 2 and 3) and those binding to syndapin (Figure 4).

Since all HA constructs containing the N-WASP PRD alone were not expressed in either COS-7 or HEK cells, we generated a GFP fusion protein of this domain. This construct was expressed successfully (Figure 4E; lysates) and used in analogous pull-down experiments with the syndapin I SH3 domain (Figure 4E). Both GFP–N-WASP and GFP–PRD interacted very well with the syndapin SH3 domain offered. In contrast, GFP remained exclusively in the supernatant. Thus, syndapins bind to the N-WASP PRD in a strong, SH3 domain-dependent and direct interaction.

Syndapin I and the syndapin II isoforms rescue the N-WASP overexpression phenotype on endocytosis

In order to examine whether the endocytosis block obtained by overexpressing PRD-containing N-WASP constructs was due to interference with syndapin functions, we tried to rescue this phenotype by syndapin co-overexpression. While expression of the PW domain of N-WASP strongly inhibited endocytic uptake of transferrin (Figures 3B and E, and 5), endocytosis was restored in cells double transfected with the PW domain and syndapin I (Figure 5), syndapin II-s (our unpublished data) or syndapin II-l (Figure 5), respectively. Endocytosis levels were restored approximately to those observed in cells overexpressing syndapin I, syndapin II-l or syndapin II-s alone. Syndapins were thus able to overcome the endocytosis block induced by the N-WASP PRD in almost all co-transfected cells. Similarly, co-overexpression of syndapin rescued the dominant-negative effect of another PRD-containing construct tested (N-WASPΔWA; our unpublished data). These data strongly implicate the syndapin–N-WASP interaction in endocytic function and suggest, furthermore, that syndapins are crucial factors for receptor-mediated endocytosis.

N-WASP is recruited to sites of high syndapin concentration

Syndapin interactions, including that with N-WASP, seem to play a crucial role in endocytosis. We therefore developed a system allowing us stably to reconstitute individual parts of the endocytic machinery at donor membranes *in vivo*. In order to be able to distinguish easily between any effects elicited and endogenous processes at the cell cortex, we used the outer mitochondrial membrane and fused syndapin cDNAs with a Flag epitope tag and the mitochondrial targeting sequence of Mas70p (Millar and

Shore, 1993). This design should lead to an insertion into the outer mitochondrial membrane in such a way that the epitope tag and the syndapin protein are accessible for proteins from the cytosol. Indeed, the syndapin constructs were targeted successfully to mitochondria (Figure 6B and D), identified by mitoTracker (Figure 6A and C) and mitoEYFP (Clontech; our unpublished data), respectively. A minor portion of syndapin fusion proteins was not targeted to mitochondria but remained associated with the actin-rich leading edge (Figure 6B, arrow).

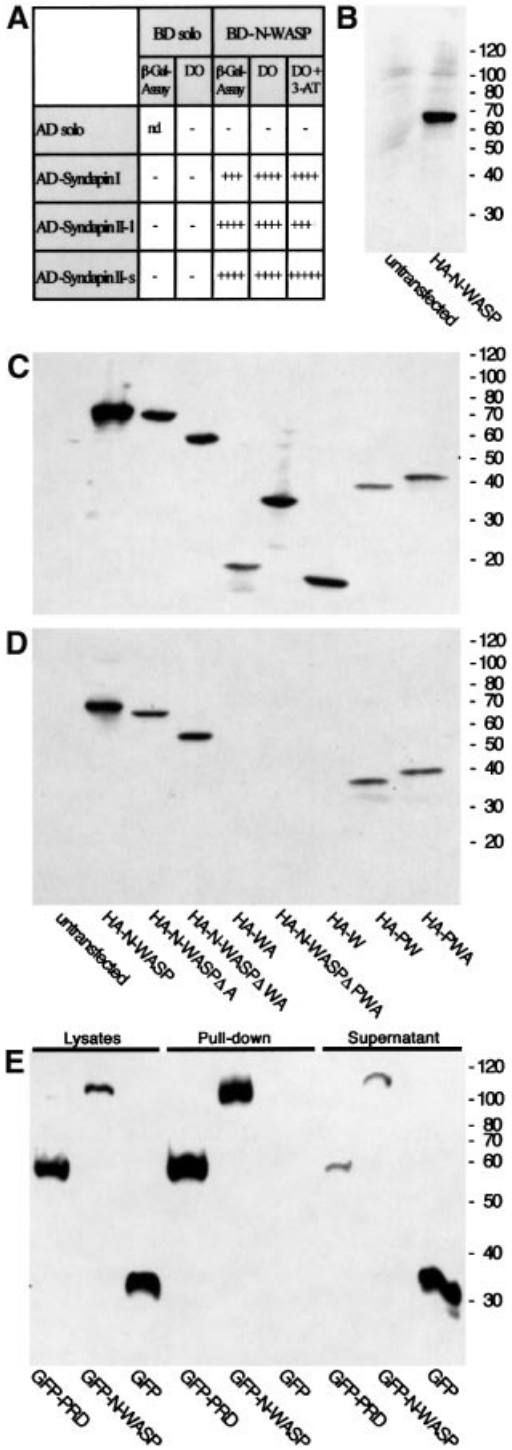

Since all prerequisites for rebuilding parts of the endocytic machinery at mitochondria seemed to be fulfilled, subsequently double transfection experiments with mito-syndapin constructs and GFP–N-WASP were performed (Figure 7). The restricted localization of mito-syndapins to mitochondria (Figure 7D and G) also led to an alteration of the cytosolic GFP–N-WASP distribution from a rather diffuse pattern, when transfected alone (Figure 7C), to a coarse punctate pattern (Figure 7F and I), which co-localized with the mito-syndapin proteins at mitochondrial membranes (Figure 7E and H). This is seen particularly well at higher magnification (Figure 7G–I). In order to prove formally that the interaction with the syndapin SH3 domain caused the observed recruitment of N-WASP, we introduced a point mutation into the SH3 domain (P434L), which impairs SH3 domain interactions (Qualmann *et al*., 1999). GFP–N-WASP did not co-localize with the mutated syndapin presented at mitochondrial membranes (Figure 7J–O). Instead, GFP–N-WASP displayed a rather diffuse localization (Figure 7L and O). The mitochondrial targeting system we designed thus proved to be a valuable tool for demonstrating that syndapins can recruit N-WASP to membranes in an SH3 domain-dependent manner *in vivo*.

Syndapin–N-WASP complexes induce actin polymerization at the sites of their formation within cells

N-WASP is an activator of the Arp2/3 complex triggering actin polymerization and it is attractive to speculate that syndapins may integrate this function into the endocytic uptake process. We therefore next analysed whether syndapin–N-WASP complexes targeted to the close vicinity of membranes would be able to promote actin polymerization at these sites (Figure 8). First, we checked whether in untransfected cells F-actin structures could be observed associated with mitochondria. In all areas of the cells, mitochondria were devoid of F-actin (Figure 8A–C). In contrast, in cells double transfected with mito-syndapin (Figure 8D) and N-WASP (Figure 8E), F-actin (Figure 8F) was observable at mitochondria at varying intensities (arrows) and we obtained a clear co-localization of all three signals (Figure 8G, arrows). Other areas, where only N-WASP was accumulated, were not necessarily positive for F-actin structures (Figure 8G).

We next asked whether it would be possible to demonstrate that the F-actin structures observed at

Fig. 4. Syndapin interacts directly with the PRD of N-WASP. (**A**) Syndapin I and II interactions with N-WASP in the yeast two-hybrid system revealed by the activation of reporter genes assayed via β-gal activity and growth on quadruple drop-out plates (DO). (**B**) Blot overlay analysis of extracts from mock-transfected and HA-tagged full-length N-WASP-transfected HEK cells with a GST fusion protein of the SH3 domain of syndapin I. (C and D) Extracts from HEK cells transiently transfected with different HA-tagged N-WASP constructs were incubated with a GST–syndapin I SH3 domain-loaded matrix. (**C**) Immunoblotting of the extracts revealed HA-tagged proteins of the expected sizes. (**D**) Analysis of proteins bound to matrix-coupled GST–syndapin I SH3 domain. Note that only HA-N-WASP constructs containing the PRD interact with GST–syndapin I SH3. (**E**) GFP fusion proteins of the PRD and of full-length N-WASP were co-precipitated efficiently by the GST–syndapin I SH3 domain.

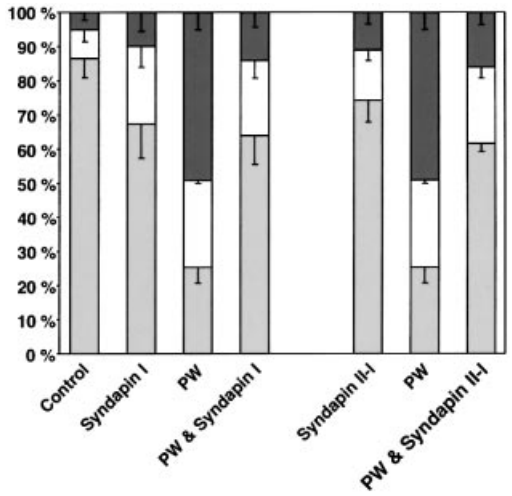

Fig. 5. Co-overexpression of syndapin I or II rescues the endocytosis block caused by overexpression of PRD-containing N-WASP fragments. Quantitation of receptor-mediated endocytosis of FITC–transferrin in COS-7 cells overexpressing full-length syndapins and the PW domains of N-WASP, and co-overexpressing syndapin and PW. Control cells, n = 333; syndapin I, n = 381; PW (N-WASP), n = 399; syndapin I and PW, n = 435; syndapin II-l, n = 341; syndapin II-l and PW, n = 337. A total of 97.4% of the HA-positive cells (stained for the HA-tagged PW domain of N-WASP) were co-expressing Xpress–syndapin I (n = 352) and 76.7% were co-expressing Xpress–syndapin II-l (n = 227), as judged by double immunofluorescence analysis.

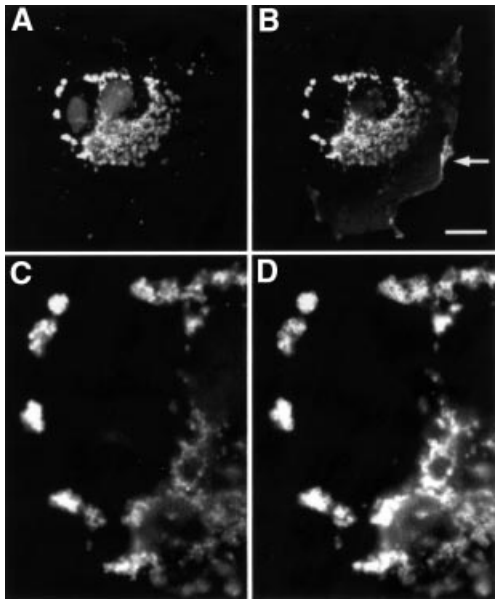

Fig. 6. Syndapin fusion proteins encompassing a mitochondrial targeting sequence are recruited efficiently to mitochondrial membranes. COS-7 cells were transfected with mito-syndapin constructs and stained with both MitoTracker® (**A** and **C**) and anti-Flag antibodies (**B** and **D**). Mito-syndapin is targeted successfully to mitochondria, as best seen in the 3.5× enlargements (C and D) of an area in (A) and (B). A small subpopulation of mito-syndapin fusion proteins can still be observed in actin-rich lamellipodia (arrow in B). Bar = 20 μm.

syndapin- and N-WASP-positive mitochondria are a consequence of the syndapin–N-WASP complexes formed at these membranes. For this purpose, we analysed the F-actin distribution in GFP–N-WASP-overexpressing cells, which we additionally transfected with mito-syndapin(P434L). In these cells, where no syndapin–N-WASP complexes are formed at mitochondria (Figure 7J–O), no F-actin structures were found at mitochondria (Figure 8H–K). Also, other cellular areas marked by a high GFP–N-WASP concentration (Figure 8I) were not necessarily distinguished by F-actin accumulation (Figure 8J). The same was true for the co-transfection of mito-syndapin and GFP–N-WASPΔPRD (Figure 8L–O). Also, cells overexpressing GFP–N-WASP alone did not display any F-actin staining at mitochondria (our unpublished data). Our analyses thus strongly suggest that the formation of F-actin structures at syndapin- and N-WASP-enriched membranes is the result of syndapin–N-WASP complexes formed at these sites.

In order to ask whether the observed F-actin formation is dependent on an activation of the Arp2/3 complex by syndapin-bound N-WASP, we overexpressed GFP–N-WASPΔWA, a construct unable to bind to the Arp2/3 complex (Figure 8P–S). The cytosolic pool of this construct was targeted successfully to mitochondria (Figure 8Q), but no F-actin was detectable there (Figure 8R). A similar result was obtained with GFP–N-WASPΔA (our unpublished data). Also, the mitochondrial build-up of F-actin induced by mito-syndapin and GFP–WASP (Figure 8D–G) was lacking in cells additionally transfected with GFP–WA (Figure 8T–W). This tool leads to an aberrant activation of the Arp2/3 complex within the cytosol but, even in cells displaying a high cytosolic F-actin content (Figure 8V), F-actin staining could not be assigned to mitochondria (Figure 8U–W).

A role for N-WASP in the endocytic uptake process

Since it appeared that syndapin–N-WASP interactions are important for endocytosis, we next asked whether it would be possible to restore endocytosis that was blocked by syndapin SH3 domains (Qualmann and Kelly, 2000), i.e. the domains interacting with N-WASP (Figure 5), by resupplying the cell with free N-WASP. As shown in Figure 9, endocytic functions of syndapin SH3 domain-overexpressing cells were restored by co-expressing N-WASP to an extent resembling that of N-WASP overexpression. In the rescue experiments, >50% of the cells showed a wild-type uptake of the fluorescent transferrin compared with <25% of the cells expressing the syndapin I SH3 domain alone. Experiments with the closely related syndapin II SH3 domain and N-WASP led to a comparable effect (our unpublished data).

The next step was to interfere with N-WASP functions directly and analyse the effects on endocytic uptake. We used two independent approaches. First, we asked whether our mitochondrial targeting system could be used for a depletion of endogenous N-WASP from the cytosol and the plasma membrane. The analysis of the localization of endogenous N-WASP in mito-syndapin-overexpressing cells (Figure 10A) showed an accumulation of N-WASP at mitochondria and reduced levels in the cytoplasm (Figure 10B). When cells overexpressing syndapin at mitochondria were analysed for uptake of transferrin, we observed a significant impairment of endocytosis; only about a third of the cells showed a wild-type uptake and each other third showed a severe reduction or a total block of uptake (Figure 10C). This effect was due mainly to SH3

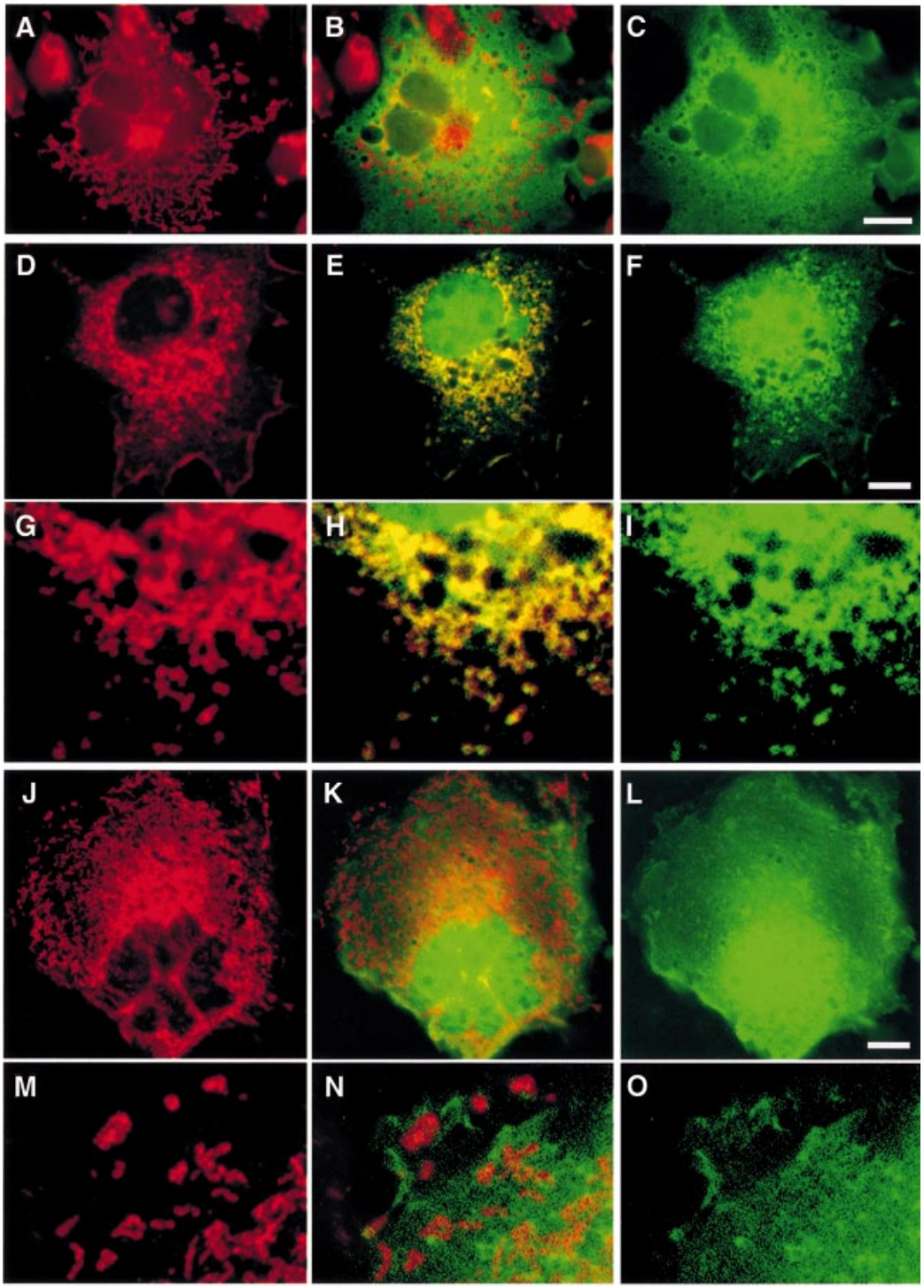

Fig. 7. N-WASP is recruited to mitochondria by mito-syndapin in an SH3 domain-dependent manner. COS-7 cells were transfected with GFP–N-WASP alone (**A–C**), with GFP–N-WASP plus mito-syndapin (**D–I**) and with GFP–N-WASP and mito-syndapin(P434L) constructs (**J–O**), respectively. Both mito-syndapin (D and G) and mito-syndapin(P434L) (J and M) detected with anti-Flag antibodies show a mitochondrial localization pattern. GFP–N-WASP is distributed diffusely and does not co-localize with mitochondria stained by MitoTracker® (A) when transfected alone (see merged image in B) but does localize to mito-syndapin-rich mitochondria (E), as seen well in the 2.7× enlarged details of (D–F) in (G–I). In contrast, in cells co-transfected with mito-syndapin(P434L) (J and M), no such recruitment is observable (K and L), as well seen in the 4× enlarged images (M–O), but GFP–N-WASP shows a rather diffuse localization (L and O). Bars = 10 μm.

domain interactions because cells overexpressing mito-syndapin II-l(P480L) only showed a slight impairment of transferrin uptake. Importantly, co-overexpression of N-WASP was able to rescue the phenotype of mito-syndapin (Figure 10C). Fewer than 10% of the cells showed a block in uptake. This rescue effect exceeded that observed for the syndapin SH3 domain (Figure 9); this is most likely to be due to the fact that the expression levels

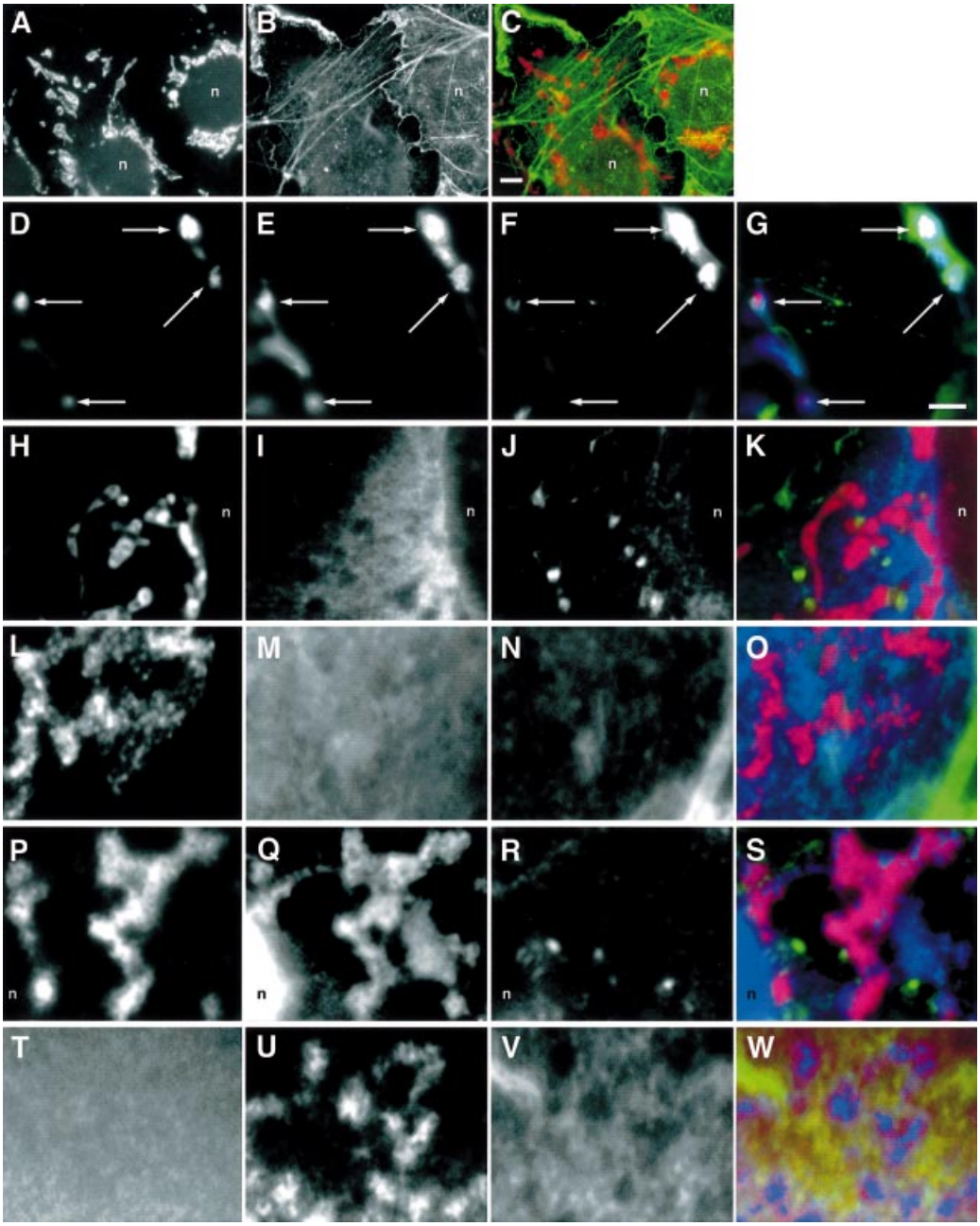

Fig. 8. Syndapin binding elicits actin polymerization at sites of intracellular N-WASP recruitment. (**A**–**C**) Untransfected cells displaying no F-actin (B) at mitochondria detected by MitoTracker® (A). (**D**–**G**) In cells double transfected with mito-syndapin (D) and GFP–N-WASP (E), F-actin (F) can be found at mitochondria (arrows). Cells transfected with mito-syndapin(P434L) and GFP–N-WASP (**H**–**K**), with mito-syndapin and GFP–N-WASPΔPRD (**L**–**O**), with mito-syndapin and GFP–N-WASPΔWA (**P**–**S**) and with a triple combination of mito-syndapin, GFP–N-WASP and HA-WA (**T**–**W**) do not show an occurrence of F-actin at mitochondria. F-actin was stained with phalloidin derivatives (B, F, J, N, R and V) and mito-syndapin by anti-Flag antibodies (D, H, L and P). The mito-syndapin staining is omitted in (T–W) and replaced by the anti-HA staining showing the diffuse distribution of HA-WA (T). In the merged images (C, G, K, O, S and W), F-actin is shown in green, GFP–N-WASP in blue and mito-syndapin, MitoTracker® and HA-WA, respectively, in red. Bar in (C) = 5 μm; bar for all other images in (G) = 2.5 μm; n, nucleus.

of mito-syndapin and N-WASP were usually well balanced; thus, no excess of N-WASP is generated, which would interfere with endocytosis.

As a second approach to interfere with N-WASP functions *in vivo*, we introduced anti-N-WASP immunoreagents into the cells using the BioPorter® system (Figure 10D). While incubations with BioPorter® alone did not lead to any impairments in endocytosis, introducing either of the two generated anti-N-WASP immunoreagents caused a strong reduction of transferrin endocytosis. As depicted in Figure 10D, the effects of the anti-N-WASP immunoreagents were dose dependent. In the subset of cells distinguished by a strong uptake of either anti-N-WASP immunoreagent (P337 or 3495), endocytosis was impaired in ~80% of the cells. Almost 40% of the cells showed a complete block of endocytosis. In cells displaying medium uptake, still only ~40% of the cells were wild-type for transferrin endocytosis, and even

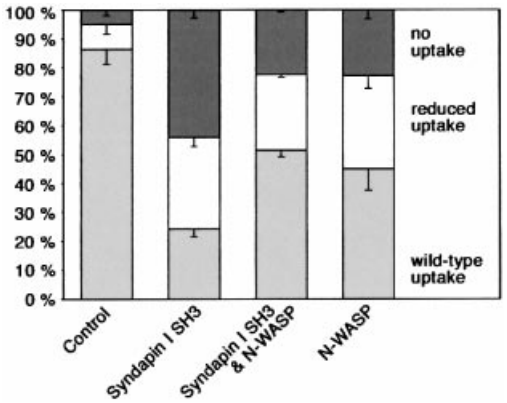

Fig. 9. Co-overexpression of N-WASP rescues the endocytosis block caused by the syndapin SH3 domain. Quantitation of receptor-mediated endocytosis of FITC–transferrin in COS-7 cells overexpressing the syndapin I SH3 domain alone and in combination with HA-N-WASP compared with control and N-WASP-transfected cells. Control, $n = 333$; Xpress–syndapin I SH3, $n = 379$; Xpress–syndapin I SH3 and N-WASP, $n = 113$; N-WASP, $n = 401$.

in cells with only weak uptake of immunoreagents endocytosis impairments were detectable (Figure 10D). The controls performed (pre-immune serum, non-immune serum and unrelated fluorescently labelled IgG uptake) failed to show any significant interferences with endocytosis but were comparable with untreated cells or cells incubated with BioPorter® alone (Figure 10D). Since interfering with N-WASP functions either by introducing antibodies against this protein or by confining it to mitochondria inhibits endocytosis and this phenotype can, furthermore, be rescued by resupplying the cells with N-WASP, we conclude that both syndapin and N-WASP play important roles at the functional interface of actin and endocytosis.

Discussion

The proteins belonging to the WASP family are multi-domain proteins, which are viewed as important components of the actin cytoskeleton because they activate the actin polymerization machinery Arp2/3 complex. We here show that overexpression of full-length N-WASP significantly inhibited endocytosis. This suggests that N-WASP interactions are involved in the endocytic uptake process. A role for mammalian WASP family members in endocytosis has also been suggested during the analysis of mice deficient for WASP. Lymphocytes from WASP knock-out mice exhibited defects in T-cell receptor endocytosis in addition to defects in actin polymerization (Zhang *et al*., 1999). The molecular basis for the endocytosis defect in these mice and the question of whether these observations represented indirect effects originating from actin cytoskeletal defects remained unaddressed. Our examinations of N-WASP interactions and their role in transferrin uptake showed that overexpression of neither the PIP_2-binding, the calmodulin-interacting nor the Cdc42-binding domain inhibited endocytosis. Several proteins implicated in different stages of clathrin-mediated endocytosis have been shown to bind PIP_2, indicating a role for PIP_2 in the sequential recruitment of clathrin coat components and accessory proteins to endocytic sites (reviewed in Cremona and De Camilli, 2001; Martin, 2001). However, in the endocytosis assays performed in this study, the PIP_2-binding N-WASP N-terminus did not act in a dominant-negative manner. The GTPase Cdc42 controlling the actin cytoskeleton has been implicated in clathrin-mediated endocytosis of IgA in polarized epithelial cells (Rojas *et al*., 2001). We examined receptor-mediated endocytosis of transferrin in non-polarized cells and did not observe any significant decrease in transferrin uptake by overexpressing the CRIB domain. Instead, we identified the PRD of N-WASP to be solely responsible for the endocytosis phenotype. We demonstrated that the syndapin SH3 domain directly binds to this N-WASP domain. We found a complete overlap of N-WASP fragments binding to syndapin and interfering with receptor-mediated endocytosis. It therefore seems likely that this protein interaction represents the molecular reason for the observed endocytosis inhibition and that the N-WASP–syndapin interaction plays an important role in endocytosis. This is strongly supported by the fact that the endocytosis block was completely rescued by co-overexpression of full-length syndapins. From these results, it can also be concluded that syndapins represent crucial components within the endocytic machinery. A role for the Arp2/3 complex activator and syndapin binding partner N-WASP in endocytosis is supported by three lines of experimental evidence presented in this study. First, the dominant-negative effect of syndapin SH3 domains can be rescued by co-expression of N-WASP, suggesting that N-WASP is a cellular target of these inhibitory tools. Secondly, we demonstrate that expressing syndapins at a defined location away from the cell cortex led to a depletion of N-WASP from the cell cortex and to dominant-negative effects on endocytosis that were rescuable by resupplying additional N-WASP molecules. Thirdly, attacking endogenous N-WASP with anti-N-WASP immunoreagents led to impairments in endocytosis.

N-WASP-triggered Arp2/3 complex-dependent actin polymerization could participate in the endocytic process at different stages. Actin polymerization could generate force facilitating the fission event, detach newly formed vesicles from the plasma membrane and/or propel them through the cytosol on actin tails (reviewed in Qualmann *et al*., 2000). Such roles of actin polymerization do not necessarily have to be essential for endocytosis, as recent examinations of the vesicle sequestration step in perforated cells suggested (Fujimoto *et al*., 2000). In support of an involvement of actin dynamics in endocytosis, intracellular vesicles were found associated with actin tails (reviewed by Taunton, 2001), and Merrifield *et al*. (2002) recently reported on small-scale actin polymerization upon endocytic vesicle formation.

In this study, we provide a possible molecular mechanism for elicitation of actin polymerization during the endocytic process: our data suggest that this could be mediated by the Arp2/3 complex activator N-WASP. N-WASP was found to interact with syndapins. We reconstituted this interaction at cellular membranes and observed local actin polymerization. Since such F-actin build-up was elicited in neither untransfected cells nor cells transfected with syndapin and N-WASP constructs incapable of interacting, but was only observed in cells

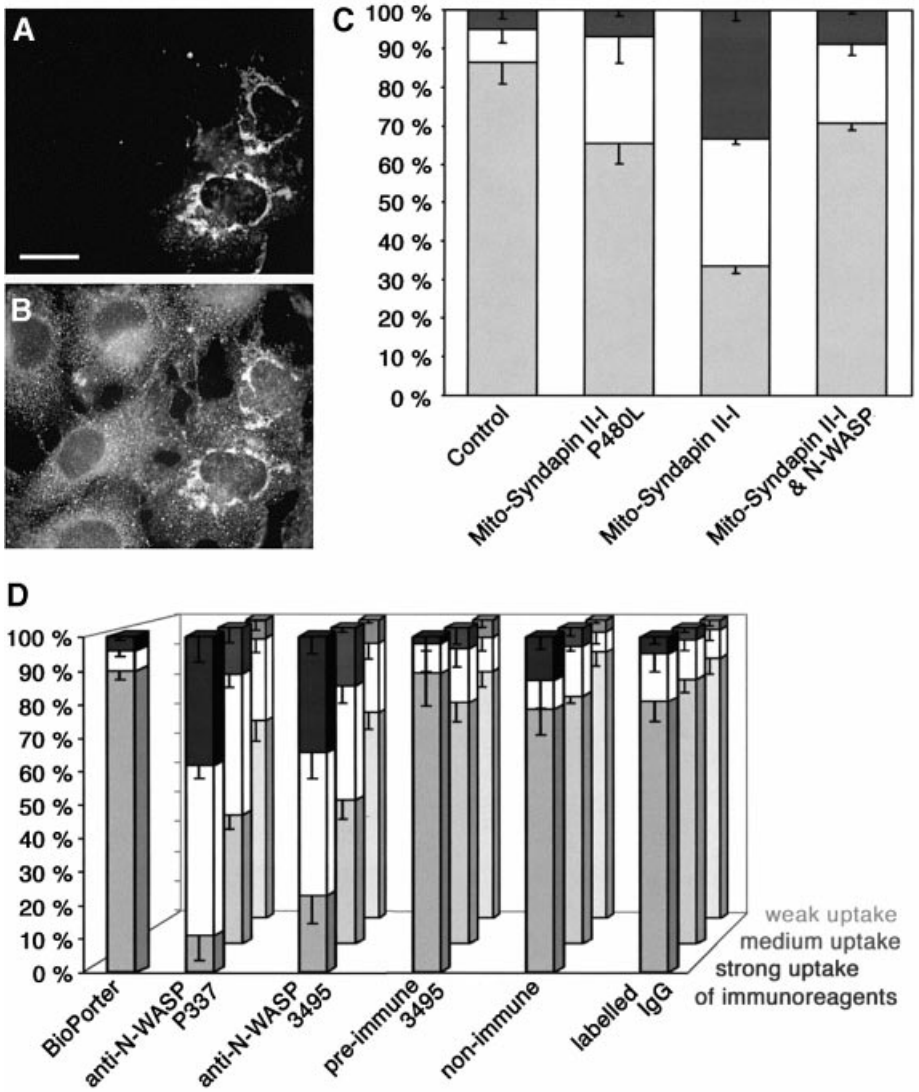

Fig. 10. Depletion of endogenous N-WASP by mitochondrial sequestration or by introduction of anti-N-WASP immunoreagents leads to endocytosis impairments. Expression of mito-syndapin (**A**) leads to a sequestration of endogenous N-WASP as detected by antibody P337 (**B**) to mitochondria. (**C**) Quantitation of receptor-mediated endocytosis of FITC–transferrin in cells overexpressing mito-syndapin II-l(P480L), mito-syndapin II-l, and mito-syndapin II-l and N-WASP. Control, $n = 333$; mito-syndapin II-l(P480L), $n = 325$; mito-syndapin II-l, $n = 326$; mito-syndapin II-l and N-WASP, $n = 216$. (**D**) Quantitation of receptor-mediated endocytosis of FITC–transferrin in cells incubated with BioPorter® to introduce immunoreagents. Depicted are the percentages of cells blocked, reduced or wild-type for endocytosis for weak (back row), medium (middle row) and strong uptake (front row) of the respective immunoreagent. Note that the two anti-N-WASP immunoreagents (P337, $n = 550$; 3495, $n = 677$) led to dose-dependent impairments of endocytosis, while BioPorter® alone ($n = 322$) as well as the three control immunoreagents (pre-immune 3495, $n = 429$; non-immune, $n = 555$; labelled IgG, $n = 670$) did not.

double transfected with mito-syndapin and GFP–N-WASP, it can be concluded that the cytoskeletal structures formed at mitochondria were a direct consequence of the reconstitution of syndapin–N-WASP complexes at these membranes. Furthermore, we observed that N-WASP constructs incapable of activating the Arp2/3 complex, although efficiently recruited, failed to give rise to F-actin structures at mitochondrial membranes. The same was observed when the Arp2/3 complex was activated aberrantly with N-WASP WA constructs within the entire cytosol. Thus, the syndapin–N-WASP-triggered actin polymerization we observed at mitochondria is Arp2/3 complex dependent as is the syndapin-induced filopodia formation (Qualmann and Kelly, 2000), suggesting that the same may be true for actin polymerization during endocytosis.

Biophysical and structural studies will be required to reveal how syndapin-triggered actin polymerization functions in detail and how it can be regulated. For the adaptor protein intersectin, it has been suggested that N-WASP binding stimulates intersectin's nucleotide exchange activity on Cdc42, which subsequently could activate N-WASP (Hussain *et al*., 2001). Interestingly, co-overexpression of N-WASP and activated Cdc42-GTP also induced actin microspikes (Miki *et al*., 1998), i.e. it shows similarities to the effect on the cortical actin cytoskeleton caused by syndapin overexpression (Qualmann and Kelly, 2000).

In the endocytic process, both a support of the fission reaction and a movement of newly formed vesicles away from the plasma membrane by cytoskeletal forces would mechanistically require (i) that actin polymerization is ignited in a polarized manner at the necks of invaginated clathrin-coated pits and (ii) that this ignition is coordinated temporally with dynamin's function in vesicle fission. Dynamin has been observed to form collars around the neck of invaginated coated pits in synaptosomes stimulated with GTPγS (Takei *et al*., 1995) and in shibire mutants at restrictive temperature (Kosaka and Ikeda, 1983). Studies in A431 cells indicated that dynamin undergoes a redistribution within clathrin lattices upon change of its nucleotide status and seems to exhibit a polarized distribution during the fission reaction (Warnock *et al*., 1997). Syndapins associate with dynamin (Qualmann *et al*., 1999; Qualmann and Kelly, 2000). As we have shown in our mitochondrial targeting experiments, syndapins also have the ability to recruit N-WASP and the associated actin polymerization machinery to sites of syndapin accumulation *in vivo*. The interaction with the dynamin-associated protein syndapin would allow a specific recruitment of N-WASP to the dynamin-rich neck of coated pits and thereby induce a polarity of actin polymerization and a directed movement of a newly formed vesicle away from the plasma membrane. In further support of the hypothesis, N-WASP has been detected specifically at the interface of vesicle membrane and actin tail of vesicles moving in *Xenopus* extracts (Taunton *et al*., 2000). Merrifield *et al*. (2002) indeed recently have observed transient actin polymerization in both spatial and temporal coordination with clathrin-coated vesicle budding at the plasma membrane by evanescent field microscopy.

Taken together, our results suggest that the cytoskeletal and endocytic functions of syndapins (Qualmann *et al*., 1999; Qualmann and Kelly, 2000) do not represent two independent aspects, but that syndapins may integrate actin cytoskeletal functions mediated via the potent Arp2/3 complex activator N-WASP into receptor-mediated endocytosis controlled by the GTPase dynamin, and that both syndapins and N-WASP perform functions important for endocytic vesicle formation.

Materials and methods

DNA constructs and recombinant proteins

Constructs encoding GST–syndapin I SH3 domain (amino acids 376–441) and Xpress-tagged mammalian syndapins were described previously (Qualmann *et al*., 1999; Qualmann and Kelly, 2000). GST fusion proteins were expressed and purified as described previously (Qualmann *et al*., 1999; Kessels *et al*., 2000).

Plasmids encoding mitochondria-targeted syndapin I and II constructs were generated by subcloning the corresponding DNA inserts from the pcDNA3.1/His vector into a derivative of the pCMV-Tag2 mammalian expression vector (Stratagene), in which the mitochondrial targeting sequence of the Mas70p protein (Millar and Shore, 1993) was inserted by PCR.

In order to generate N-WASP expression constructs, DNA fragments corresponding to the regions of rat N-WASP depicted in Figure 2A were amplified by PCR and cloned into a derivative of the pEGFP vector (Clontech), in which GFP was replaced by the HA peptide. Additional PCR-generated N-WASP constructs used for biochemical analyses include GFP–PRD (amino acids 265–391), HA-N-WASPΔA (amino acids 1–481) and HA-WA (amino acids 391–501). GFP–N-WASP and GFP–N-WASPΔWA were generated by subcloning from the above HA-N-WASP constructs, and GFP–N-WASPΔPRD (lacking amino acids 265–390) was generated by PCR. All of these constructs were analysed by DNA sequencing.

Antibodies

Polyclonal anti-N-WASP antibodies were raised in guinea pig (P337) and in rabbit (3495) (Alpha Diagnostic Intl, Inc.) against a purified GST fusion protein of amino acids 118–273 of rat N-WASP. Antibodies were depleted against GST and subsequently affinity purified on GST–N-WASP (amino acids 118–273) blotted to nitrocellulose membranes. Rabbit anti-syndapin I antibodies (2704) and anti-GST antibodies were described previously (Qualmann *et al*., 1999). Monoclonal anti-Flag antibodies (M2) and anti-synaptophysin antibodies were from Sigma, monoclonal anti-GFP (B34) and anti-HA (HA.11) antibodies were from Babco, and monoclonal anti-Xpress antibodies were purchased from Invitrogen.

Secondary antibodies used in this study include goat anti-mouse–peroxidase (Dianova), goat anti-rabbit–peroxidase (Dianova), goat anti-guinea pig–peroxidase (ICN), fluorescein isothiocyanate (FITC)-conjugated goat anti-guinea pig (ICN), rhodamine-conjugated goat anti-guinea pig (ICN), Alexa Fluor™ 568–goat anti-mouse (Molecular Probes), Alexa Fluor™ 568–goat anti-rabbit (Molecular Probes), Alexa Fluor™ 350–goat anti-mouse (Molecular Probes) and Alexa Fluor™ 488–goat anti-rabbit (Molecular Probes).

Blot overlay and co-precipitation assays

HEK293 cells were transfected with different GFP- and HA-tagged constructs using the LipofectAMINE PLUS transfection reagent method according to the manufacturer's instructions (Gibco). Immobilized GST–syndapin I SH3 domain was incubated with high speed supernatants prepared from the lysed HEK cells (Kessels *et al*., 2001) overnight at 4°C. Material specifically co-precipitated with the syndapin SH3 domain was analysed by SDS–PAGE and immunoblotting with anti-HA and anti-GFP antibodies, respectively. Blot overlay experiments were performed with GST–syndapin I SH3 domain on HEK293 cell extracts transfected with HA-full length N-WASP or untransfected according to the procedure described previously (Qualmann *et al*., 1999).

Tissue fractionation

Tissue fractionation was carried out essentially as described by Carlin *et al*. (1980) with modifications according to tom Dieck *et al*. (1998). A 10 μg aliquot of protein of each fraction was loaded on 5–20% polyacrylamide gels and the subcellular protein distribution was analysed by immunoblotting.

Yeast two-hybrid analyses

The GAL4-based MATCHMAKER yeast two-hybrid system 3 (Clontech) was used to address an interaction between N-WASP and different syndapin isoforms and splice variants *in vivo*. For this purpose, the full-length open reading frame of rat N-WASP was inserted in-frame behind the DNA-binding domain of yeast Gal4 encoded by the pGBTK7 vector (BD–N-WASP), and full-length syndapin I, syndapin II-s and syndapin II-l were subcloned into the pGADT7 vector in-frame with the activation domain (AD–syndapins). Yeast strain Y187 was transformed with BD–N-WASP and with the pGBTK7 vector encoding the BD domain alone. Yeast strain AH109 was transformed with pGADT7, AD–syndapin I, AD–syndapin II-l and AD–syndapin II-s. Yeast matings and selection of diploids were performed according to the manufacturer's instructions. Reporter gene activity was assayed by a β-galactosidase filter assay and by checking the ability of the colonies to grow on SD plates lacking L-leucine, L-tryptophan, L-histidine and adenine (quadruple drop-out; DO). For a more stringent selection, colonies were restreaked additionally onto DO plates including 1 mM 3-amino-1,2,4-triazole (3-AT) in order to inhibit low levels of leaky expression of His3p.

Cell culture and immunofluorescence microscopy

HEK293 and COS-7 cells were maintained in Dulbecco's modified Eagle's medium containing 10% fetal bovine serum. Primary hippocampal cultures were prepared and grown on poly-D-lysine-coated glass coverslips as described (Kessels *et al*., 2001).

Cells were fixed in 4% paraformaldehyde in phosphate-buffered saline (PBS) pH 7.4 containing 0.9 mM $CaCl_2$ and 0.5 mM $MgCl_2$ for 15 min at room temperature and processed for immunofluorescence according to Kessels *et al*. (2001). For mitochondrial staining, cells were incubated with MitoTracker® Red CMXRos (Molecular Probes) at a final concentration of 0.2 μM in medium at 37°C for 20 min, washed and then fixed. F-actin was stained with Texas red–phalloidin or Alexa

Fluor™ 488–phalloidin (Molecular Probes). Images were recorded digitally using a Leica DMRD fluorescence microscope and a Leica TCS NT laser confocal microscope with a Leica TCS software package, and processed using Adobe Photoshop software.

Transferrin uptake assays

COS-7 cells were subjected to transferrin uptake assays 48 h after transfection as described previously (Qualmann and Kelly, 2000; Kessels *et al*., 2001). COS-7 cells treated with BioPorter® to introduce immunoreagents were subjected to endocytosis assays 5 h after the start of treatment. The BioPorter® uptake of immunoreagents was performed according to the manufacturer's instructions (Gene Therapy Systems, Inc.) followed by a 1 h recovery period (addition of 1 vol. of serum-containing medium). The percentages of transfected cells showing no detectable uptake of transferrin, significantly reduced transferrin signals and normal levels of internalized transferrin, and SDs, were calculated by scoring and counting cells in ⩾3 independent experiments each.

For the rescue experiments of the N-WASP PRD overexpression phenotype, cells were double transfected with N-WASP constructs and Xpress-tagged full-length syndapin. Due to the lower expression rates of the HA-tagged N-WASP constructs compared with Xpress-tagged syndapin (determined by double labelling of both epitope tags, our unpublished data), anti-HA immunostainings were used to identify double-transfected cells for the endocytosis quantifications. In some cases, triple labellings were also used. For the rescue experiments of the phenotypes caused by syndapin SH3 domains and mito-syndapin, exclusively triple labellings were used.

Acknowledgements

We thank H.Miki for rat N-WASP cDNA, Kathrin Hartung for her technical assistance, and the students Tilman Boicher, Sven Peters and Nicole Jäger for their assistance. We are very grateful to Eckart Gundelfinger for his support. This work was supported by grants from the Deutsche Forschungsgemeinschaft (Qu 116/2-1, Qu 116/2-3 and Ke 685/2-1) and from the Kultusministerium Land Sachsen-Anhalt (3199A/0020G).

References

Brodin,L., Löw,P. and Shupliakov,O. (2000) Sequential steps in clathrin-mediated synaptic vesicle endocytosis. *Curr. Opin. Neurobiol.*, **10**, 312–320.

Carlin,R.K., Grab,D.J., Cohen,R.S. and Siekevitz,P. (1980) Isolation and characterization of postsynaptic densities from various brain regions: enrichment of different types of postsynaptic densities. *J. Cell Biol.*, **86**, 831–845.

Cremona,O. and De Camilli,P. (2001) Phosphoinositides in membrane traffic at the synapse. *J. Cell Sci.*, **114**, 1041–1052.

Fujimoto,L.M., Roth,R., Heuser,J.E. and Schmid,S.L. (2000) Actin assembly plays a variable, but not obligatory role in receptor-mediated endocytosis in mammalian cells. *Traffic*, **1**, 161–171.

Higgs,H.N. and Pollard,T.D. (1999) Regulation of actin polymerization by Arp2/3 complex and WASp/Scar proteins. *J. Biol. Chem.*, **274**, 32531–32534.

Hussain,N.K. *et al*. (2001) Endocytic protein intersectin-l regulates actin assembly via Cdc42 and N-WASP. *Nat. Cell Biol.*, **3**, 927–932.

Kessels,M.M., Engqvist-Goldstein,Å.E.Y. and Drubin,D.G. (2000) Association of mouse actin-binding protein 1 (mAbp1/SH3P7), an Src kinase target, with dynamic regions of the cortical actin cytoskeleton in response to Rac1 activation. *Mol. Biol. Cell*, **11**, 393–412.

Kessels,M.M., Engqvist-Goldstein,Å.E.Y., Drubin,D.G. and Qualmann,B. (2001) Mammalian Abp1, a signal-responsive F-actin-binding protein, links the actin cytoskeleton to endocytosis via the GTPase dynamin. *J. Cell Biol.*, **153**, 351–366.

Kosaka,T. and Ikeda,K. (1983) Possible temperature-dependent blockage of synaptic vesicle recycling induced by a single gene mutation in *Drosophila*. *J. Neurobiol.*, **14**, 207–225.

Martin,T.F.J. (2001) PI(4,5)P_2 regulation of surface membrane traffic. *Curr. Opin. Cell Biol.*, **13**, 493–499.

Merrifield,C.J., Feldman,M.E., Wan,L. and Almers,W. (2002) Imaging actin and dynamin recruitment during invagination of single clathrin-coated pits. *Nat. Cell Biol.*, **4**, 691–698.

Miki,H., Miura,K. and Takenawa,T. (1996) N-WASP, a novel actin-depolymerizing protein, regulates the cortical cytoskeletal rearrangement in a PIP_2-dependent manner downstream of tyrosine kinases. *EMBO J.*, **15**, 5326–5335.

Miki,H., Sasaki,T., Takai,Y. and Takenawa,T. (1998) Induction of filopodium formation by a WASP-related actin-depolymerizing protein N-WASP. *Nature*, **391**, 93–96.

Millar,D.G. and Shore,G.C. (1993) The signal anchor sequence of mitochondrial Mas70p contains an oligomerization domain. *J. Biol. Chem.*, **268**, 18403–18406.

Plomann,M. *et al*. (1998) PACSIN, a brain protein that is upregulated upon differentiation into neuronal cells. *Eur. J. Biochem.*, **256**, 201–211.

Qualmann,B. and Kelly,R.B. (2000) Syndapin isoforms participate in receptor-mediated endocytosis and actin organization. *J. Cell Biol.*, **148**, 1047–1061.

Qualmann,B. and Kessels,M.M. (2002) Endocytosis and the cytoskeleton. *Int. Rev. Cytol.*, **220**, 93–144.

Qualmann,B., Roos,J., DiGregorio,P.J. and Kelly,R.B. (1999) Syndapin I, a synaptic dynamin-binding protein that associates with the neural Wiskott–Aldrich syndrome protein. *Mol. Biol. Cell*, **10**, 501–513.

Qualmann,B., Kessels,M.M. and Kelly,R.B. (2000) Molecular links between endocytosis and the actin cytoskeleton. *J. Cell Biol.*, **150**, F111–F116.

Riezman,H., Munn,A., Geli,M.I. and Hicke,L. (1996) Actin-, myosin- and ubiquitin-dependent endocytosis. *Experientia*, **52**, 1033–1041.

Rojas,R., Ruiz,W.G., Leung,S.-M., Jou,T.-S. and Apodaca,G. (2001) Cdc42-dependent modulation of tight junctions and membrane protein traffic in polarized Madin–Darby canine kidney cells. *Mol. Biol. Cell*, **12**, 2257–2274.

Schmid,S.L. (1997) Clathrin-coated vesicle formation and protein sorting: an integrated process. *Annu. Rev. Biochem.*, **66**, 511–548.

Simpson,F., Hussain,N.K., Qualmann,B., Kelly,R.B., Kay,B.K., McPherson,P.S. and Schmid,S.L. (1999) SH3-domain-containing proteins function at distinct steps in clathrin-coated vesicle formation. *Nat. Cell Biol.*, **1**, 119–124.

Slepnev,V.I. and De Camilli,P. (2000) Accessory factors in clathrin-dependent synaptic vesicle endocytosis. *Nat. Rev. Neurosci.*, **1**, 161–172.

Takei,K., McPherson,P.S., Schmid,S.L. and De Camilli,P. (1995) Tubular membrane invaginations coated by dynamin rings are induced by GTP-γS in nerve terminals. *Nature*, **374**, 186–190.

Taunton,J. (2001) Actin filament nucleation by endosomes, lysosomes and secretory vesicles. *Curr. Opin. Cell Biol.*, **13**, 85–91.

Taunton,J., Rowning,B.A., Coughlin,M.L., Wu,M., Moon,R.T., Mitchison,T.J. and Larabell,C.A. (2000) Actin-dependent propulsion of endosomes and lysosomes by recruitment of N-WASP. *J. Cell Biol.*, **148**, 519–530.

tom Dieck,S. *et al*. (1998) Bassoon, a novel zinc-finger CAG/glutamine-repeat protein selectively localized at the active zone of presynaptic nerve terminals. *J. Cell Biol.*, **142**, 499–509.

Warnock,D.E., Baba,T. and Schmid,S.L. (1997) Ubiquitously expressed dynamin-II has a higher intrinsic GTPase activity and a greater propensity for self-assembly than neuronal dynamin-I. *Mol. Biol. Cell*, **8**, 2553–2562.

Zhang,J. *et al*. (1999) Antigen receptor-induced activation and cytoskeletal rearrangement are impaired in Wiskott–Aldrich syndrome protein-deficient lymphocytes. *J. Exp. Med.*, **190**, 1329–1342.

Received April 15, 2002; revised August 20, 2002; accepted September 23, 2002